Vegetable Research

ARTICLE

Open Access

https://doi.org/10.48130/vegres-0025-0049

Vegetable Research **2026**, 6: e007

Deciphering the functional characterization of *Orange* (*Or*) genes during development and ripening of watermelon (*Citrullus lanatus*) fruit

Chenghong Zeng[1#], Putao Wang[1,2#], Cong Zhou[1], Sikandar Amanullah[3], Pengcheng Zeng[1], Yufei Tang[1], Qinghong Zhou[1] and Qianglong Zhu[1*]

[1] *Jiangxi Province Key Laboratory of Vegetable Cultivation and Utilization, Jiangxi Agricultural University, Nanchang, Jiangxi 330045, China*

[2] *Key Laboratory of Dong Medical Research of Hunan Province, Biomedical Research Institute, Hunan University of Medicine, Huaihua, Hunan 418000, China*

[3] *Department of Horticultural Science, North Carolina State University, Mountain Horticultural Crops Research and Extension Center, 455 Research Drive, Mills River, NC 28759, USA*

[#] Authors contributed equally: Chenghong Zeng, Putao Wang

[*] Correspondence: longzhu2011@126.com (Zhu Q)

Abstract

Carotenoids are the main nutrients and coloring matter in the flesh of watermelon. However, the significant role of *Orange* gene in carotenoid accumulation and chromoplast differentiation remains uncharacterized in watermelon. In this study, the *ClOr1* gene was obtained through homologous alignment, identified to be highly expressed in the red-fleshed watermelon LSW-177, and significantly associated with carotenoid content. A single-nucleotide polymorphism in the *ClOr1* gene was detected and confirmed to distinguish well between white-fleshed and non-white-fleshed watermelon after cloning the *ClOr1* from LSW-177 and W1-60, and aligning 428 germplasm resources of watermelon, which suggested that the *ClOr1* could be taken as a key candidate gene to promote carotenoid accumulation in watermelon fruit flesh. Transient expression assay similarly revealed that ClOr1 is localized to the nucleus, and overexpression of *ClOr1* accelerated fruit coloration by contributing a 1.8- to 19.2-fold increase of total carotenoid content in transgenic tomato lines. Furthermore, the *ClOr1* gene silencing resulted in a prominent reduction in carotenoid accumulation in the fruits of LSW-177 using virus-induced gene silencing. A direct protein-protein interaction was identified between ClOr1 and ClPSY1 by Y2H and BiFC assays, and *ClPSY1* was exhibited as a key gene based on its significant expression related to carotenoid content in the experimental materials. Hence, these results suggested that the ClOr1 plays a positive role in regulating carotenoid accumulation during development and ripening in watermelon fruit by increasing the activities of ClPSY1 protein.

Citation: Zeng C, Wang P, Zhou C, Amanullah S, Zeng P, et al. 2026. Deciphering the functional characterization of *Orange* (*Or*) genes during development and ripening of watermelon (*Citrullus lanatus*) fruit. *Vegetable Research* 6: e007 https://doi.org/10.48130/vegres-0025-0049

Introduction

Watermelon (*Citrullus lanatus*) is one of the important horticultural crops in the genus Citrullus of the family Cucurbitaceae. Its fruit is rich in nutrients that are necessary for maintaining human health, such as carotenoids, vitamins, glucose, amino acids, and so on[1]. Among them, carotenoids and their derivatives have important roles in preventing cancer, reducing the risk of cardiovascular disease, alleviating eye diseases, and regulating the immune system[2].

In higher plants, carotenoids are crucial for photosynthesis, serve as precursors for ABA biosynthesis, and are the main dietary source of vitamin A precursors in human diets[3]. More than 750 carotenoids have been identified and are widely distributed in colorful flowers, fruits, leaves, and roots[4]. Carotenoids such as β-carotene[3], lycopene[2], and lutein[5] play important roles in the food and pharmaceutical industries because of their antioxidant activity. Carotenoids are important nutrients and color-presenting substances in the flesh of watermelon[6]. The regulatory mechanism is still not completely clear; therefore, further exploration will be helpful to comprehensively understand carotenoid metabolism and improve the fruit nutrition in watermelon.

Even though the metabolic pathway of carotenoids has been explored in many important plants[7], the metabolic process is still very complicated. Under the interaction of genotype and environment, it has been noticed that the carotenoid metabolic process is mainly regulated by transcriptional level[8], transcription factor[9], post-transcriptional level[10,11], post-translational level[12,13], and epigenetic modification[14,15]. Post-transcriptional regulation plays an essential role in regulating the levels and activities of enzymes related to carotenoid synthesis in plants, and especially during fruit development and ripening, such as the direct interaction of SlSGR1 protein with SlPSY1 protein in tomato, which regulates carotenoid accumulation in fruits[10]. Nudix hydrolase 23 (NUDX23), a Nudix domain-containing protein, regulates carotenoid biosynthesis by directly interacting with PSY and GGPPS in chloroplasts, thereby enhancing the stability of PSY and GGPPS proteins in the large PSY-GGPPS enzyme complex[16]. A *CmOr* nonsense mutation (*Cmor-lowβ*) was identified in the EMS-induced low-β mutant in melon, which significantly reduced PSY protein levels and enzyme activity, leading to a decrease in carotenoid metabolic flux and accumulation[17]. The interaction between CmOR family proteins and light-harvesting chlorophyll a-b binding proteins pointed to a previously unrecognized role of CmOR in maintaining chloroplast function in melon fruit[13]. CmOR protein interacts with the carotenoid sequestration protein CmFBN1 protein, which stimulates plastoglobule proliferation and promotes the accumulation of β-carotene in the chloroplasts of melon fruit[18]. PSY, serving as the rate-limiting enzyme in catalyzing carotenoid metabolism, influenced the content of carotenoids[7]. According to previous reports, the expression of *ClPSY1* in the red-fleshed watermelon was significantly higher than that in other flesh-colored watermelons, and it regulated carotenoid accumulation and chromoplast differentiation[19].

The *Or* gene, as one of the important genes that can regulate the differentiation of chromoplasts, was a significant factor in regulating the metabolism and accumulation of carotenoids in plants[20,21]. The *Or* gene was initially found in cauliflower mutants, and mutations of the *Or* gene led to the accumulation of large quantities of β-carotene in the weakly or unpigmented tissues, such as floral bulbs, the pith, the base of the leaves, the phloem, and the bud meristems, which turned into an orange color[22]. The *Or* gene encodes a class of DnaJ-like zinc finger protein-containing structural domains whose function is related to triggering the formation of chromoplasts from proplastids or other noncolored plastids to accumulate carotenoids[20]. Except in melon, ectopic expression of the alfalfa (*Medicago sativa* L.) *Or* gene also increased carotenoid accumulation and plant tolerance to drought stress[23]. Furthermore, AtOr (At5g61670) drove the conversion of proplastids or other noncolored plastids into chromoplasts, thereby enhancing carotenoid storage[24]. High expression of $AtOr^{WT}$ and $AtOr^{His}$ in tomato promoted overall early flowering and more fruit and seed number in tomato[25]. Overexpression of the *Or* gene in sweet potato (*Ipomoea batatas* [L.] Lam) promoted carotenoid accumulation and abiotic stress tolerance in storage roots[26]. The *OR* homolog *BrGOLDEN* likely enhanced carotenoid accumulation by modulating the expression of key carotenoid biosynthesis genes, including *ZEP*, *DXS*, *CYP97C1*, and *PSY* in *Brassica rapa*[27]. Overexpression of either potato *StOR* or $StOR^{His}$ regulated carotenoid homeostasis and improved plant adaptation to environmental stress[28]. An integration analysis of carotenoids and transcriptome during the development of five different flesh-colored watermelon fruits indicated that the *Cla018406* gene (a chaperone protein dnaJ-like protein) may be a candidate gene for β-carotene accumulation in a previous study, *Cla018406* was homologous to the *BoOr*[20] and *CmOr*[21], and its gene expression pattern was related to the β-carotene content abundant in orange flesh[6]. However, the *Or* gene function in regulating carotenoid synthesis and accumulation during fruit development and ripening is still unknown and needs further verification in watermelon.

Herein, this research aimed to decipher the *Or* gene family and functionally verify the key gene regulating carotenoid synthesis and accumulation during fruit development and ripening in watermelon. The carotenoid metabolism analysis, gene expression, genetic transformation, virus-induced gene silencing (VIGS), yeast two-hybrid assay (Y2H), and bimolecular fluorescent complimentary assay (BiFC) were used to determine the gene function and molecular mechanism of *ClOr*. The retrieved results will provide an insight into the verification of the *ClOr* gene that regulates carotenoid synthesis and accumulation during development and ripening in watermelon fruits, with the hope of promoting the genetic improvement of watermelon fruit flesh based on the *ClOr* gene in the future.

Materials and methods

Plant materials and growth conditions

The two watermelon varieties (LSW-177 [*Citrullus lanatus*] and W1-60 [*Citrullus amarus*]) were selected as experimental materials. The mature flesh of the LSW-177 watermelon was red, while the mature flesh of the W1-60 watermelon was white. They were cultivated at the Horticultural Teaching and Experimental Base of Jiangxi Agricultural University. All plants were grown under standardized field conditions with uniform agronomic practices.

The tobacco (*Nicotiana benthamiana*) was used for subcellular localization assays; its seedlings were grown in autoclaved potting mix within a well-protected climate-controlled condition of greenhouse (24/20 °C day/night cycle, 16 h photoperiod supplemented with artificial lighting) for 30 d post-germination to inject.

The seeds of tomato (*Solanum lycopersicum* L. cv. Micro-Tom) were obtained from Wuhan Boyuan, China. After complete expansion of the cotyledons, they were excised and used for Agrobacterium-mediated transformation. The seeds of LSW-177 for VIGS were cultured under controlled greenhouse conditions prior to infiltration.

Carotenoid extraction and quantification

The fruit flesh samples were collected from five developmental stages at days after pollination (DAP) of red- and white-fleshed watermelons (e.g., 10, 18, 26, 34, and 42 DAP) and freeze-dried. Then, samples were finely ground using a freeze-mixer grinder (30 Hz, 1 min); 50 mg of fruit flesh powder was sampled, and 0.5 mL of a hexane/acetone/ethanol mixture (1:1:1) containing 0.01% BHT (Butylated Hydroxytoluene, g/mL) was added in equal volume ratios, which was fully extracted by vortexing at 2,800 rpm in a vortex mixer (30 s) and aided with an ultrasonic cleaner. The carotenoids were fully extracted by vortex mixer at 2,800 rpm (30 s) and ultrasonic cleaner-assisted dissolution (40 kHz, 20 min); the obtained extract was centrifuged for 5 min (12,000 rpm, 4 °C) to obtain the supernatant, which was repeated once and combined; the supernatant was concentrated by vacuum centrifugal concentrator (1,400 rpm, 6 h), then reconstituted with 100 μL of an equal-volume ratio of methanol/methyl tert-butyl ether, and filtered by a 0.22 μm filter membrane. The solution was filtered through a 0.22 μm membrane into a brown vial and analyzed by Liquid Chromatography-Tandem Mass Spectrometry (LC-MS/MS) to detect the compositions and contents of carotenoids in the flesh.

The flesh samples of watermelon and tomato were finely ground using a freeze-mixer grinder (30 Hz, 1 min); carotenoid measurements were done by following the method described by Rodriguez et al.[29]. In brief, 4 mL of 95% ethanol (FW, 0.2 g) was extracted under light for 20 min at 4 °C, and at 12,000 rpm for 5 min to obtain the supernatant; the extraction was repeated for the precipitate; the supernatant was mixed and concentrated using a vacuum centrifugal concentrator and re-dissolved with 1 mL of 95% ethanol; and the absorbance was measured using a microplate reader at 665, 649, and 470 nm. The formula for carotenoid content was calculated using the method described by Arnon[30].

Microscopic observation of watermelon flesh

The freshly harvested fruits were brought back to the laboratory, and the longitudinal sections of the fruits were photographed to record the fruit development process; 2–3 cm^2 of the center flesh was taken and submerged in FAA fixative (Formaldehyde-acetic acid-ethanol fixative, containing 38% formaldehyde 5 mL, acetic acid 5 mL, 70% ethanol 90 mL, and 5 mL of glycerol) for 1 h, and then the flesh was transferred to 0.1 M Na_2-EDTA solution (pH = 9) in a 60 °C hot water bath for 150 min to promote intercellular segregation. After ending the flesh treatment, a small amount of flesh tissue was scraped with a razor blade to observe the chromoplast in the flesh cells under the optical microscope. The submicroscopic structure in the flesh cells was observed using a transmission electron microscope (TEM) according to a previous study[19].

Identification of the *Or* gene family in watermelon

The protein database (v2.5) of watermelon genome (97103) from the CuGenDBv2 (http://cucurbitgenomics.org/v2) was selected as

the subject database, the amino acid sequence of the *AtOr* gene (At5g61670) was obtained from NCBI (www.ncbi.nlm.nih.gov), the amino acid sequence of the *AtOr* gene was blasted, and the homolog of the *Or* gene family members of watermelon were obtained (E-value < 1e-10, Identity > 60%). Then, the nucleotide sequence and amino acid sequences of the ClOr were obtained from CuGenDBv2, and their gene structures were analyzed using CSDS (v2.0) (http://gsds.gao-lab.org/).

For multiple sequence alignment and phylogenetic tree analysis, the amino acid sequences of the *Or* proteins of 14 other species were downloaded from the NCBI database, and their accessions are listed in Supplementary Table S1. Multiple sequence alignment of the 16 Or proteins was performed by MEGA software (v11), and the results were demonstrated using DNAMAN software (v9.0). The phylogenetic tree was constructed by the ML method (Maximum likelihood) with 1,000 bootsteps and visualized using Chiplot (www.chiplot.online/).

Gene cloning and dCAPS molecular marker development

Total RNA was extracted from 34 DAP flesh samples of red- and white-fleshed watermelon using the MolPure® Plant RNA Kit (Yeasen, Shanghai, China). The purified total RNA was reverse-transcribed into cDNA using the PrimeScript™ RT reagent Kit with gDNA Eraser (Takara, Shiga, Japan), and amplification of full-length *ClOr1* cDNA with gene-specific primers was performed by polymerase chain reaction (PCR). All the PCR products were then inserted into pClone007 Versatile Simple Vector (Tsingle, Beijing, China) and transformed into *Trelief*™ 5α Chemically Competent Cell (Tsingle, Beijing, China). In addition, a dCAPS molecular marker based on the SNP in ClOr1 was developed to distinguish between white-fleshed and non-white-fleshed watermelons. The total DNA was extracted from 34 DAP leaves of red- and white-fleshed watermelon using the MolPure® Plant Plus DNA Kit (Yeasen, Shanghai, China). For molecular genotyping, the PCR amplifications were performed using 2 × Hieff Canace® Plus PCR Master Mix (Yeasen, Shanghai, China), then the PCR products were digested with suitable restriction enzymes (Hpy166II, NEBiolabs, Beijing, China), and recognizing dCAPS sites. The information of developed primers is shown in Supplementary Table S2. The web server program SOPMA was used to analyze the secondary structure of proteins predicted by ClOr1^{Trp} and ClOr1^{Cys}, and the Swiss Model was used for online prediction of their tertiary structure.

Subcellular location

To confirm where *ClOr1* is expressed in cells. Homologous recombination and the Golden Gate seamless cloning method (*Bsa* I/*Eco* 31I) were used to construct the pBWA(V)HS-Osgfp-ClOr1 fusion vector. The primers used for the fusion vector are listed in Supplementary Table S2, together with the cytosolic Marker plasmid to transform the GV3101 Competent cell, respectively. Successfully transformed Agrobacterium was cultured in the bacterial fluid OD_{600} = 0.6, centrifuged at 5,000 rpm (4 min) to obtain the bacterium and resuspended, and injected pBWA(V)HS-Osgfp-ClOr1 into the tobacco leaves by mixing with the Agrobacterium plasmid in the ratio of 1:1 with the cytosolic Marker plasmid. Two days later, Fluorescence images of GFP were observed under a confocal microscope and photographed for documentation.

Genetic transformation of *ClOr1* in tomato

The pBWA(V)KS-ClOr1-Osgfp fusion vector was constructed by the homologous recombination and Golden Gate seamless cloning method using restriction endonuclease (*Bsa* I/*Eco* 31I). The primers used for vector construction are shown in Supplementary Table S2. Subsequently, the fusion vector was converted to the Agrobacterium GV3101 strain using the freeze-thaw method. For tomato transformation, tomato cotyledons were infiltrated with Agrobacterium resuspension with OD_{600} = 0.2 for 10 min, and kanamycin resistance was used to screen the healing wounds. The screened healing wounds were inoculated into the differentiation medium for 30 d. After the differentiated seedlings grew to about 2–3 cm, they were cut off from the healing wounds and inoculated into the rooting medium for 10 d. After the development of a proper root system, the seedlings were transferred and cultivated in sterilized substrate (24/20 °C, 16 h light/8 h dark). The insertion of *ClOr1* in the OE tomatoes was verified using the MolPure® Plant Plus DNA Kit (Yeasen, Shanghai, China).

VIGS assay for silencing the *ClOr1* gene

To obtain a specific sequence of the *ClOr1* gene for VIGS, SsClOr1 was designed using an online tool (https://vigs.solgenomics.net) and inserted into plasmid pTRV2. Gene-specific primers containing restriction sites (*Xba* I and *Bam*H I) were designed for amplification (Supplementary Table S2). The recombinant vector and empty vector were transformed into GV3101, respectively. According to the method reported in a previous study[31], cultivate Agrobacterium GV3101 to an OD_{600} of 1.0, then thoroughly mix the pTRV1 with the pTRV2 and pTRV2-SsClOr1 in a 1:1 ratio for the control group and experimental group, respectively. After incubating in the dark for three hours, select three fruits (18 DAP) from the potted watermelons of the LSW-177 in the greenhouse. A total of 1 mL of the mixed infestation solution of the control group and experimental group was injected into two opposite sides of the middle fruit using a 1 mL sterile syringe. Infection was repeated on the third and sixth days after the first injection, and fruit flesh tissue near the needle insertion site was collected 3 d after the third injection.

Validation of interaction between ClOr1 and ClPSY1

The Y2H and BiFC assays were used to validate the interaction between ClOr1 and ClPSY1. For the Y2H assay, the full-length *ClOr1* CDS was fused into the pGBKT7 vector (BD), forming the BD-ClOr1 fusion vector, whereas the full-length *ClPSY1* (Cla97C01G008760) CDS was fused into the pGADT7 vector (AD), forming the AD-ClPSY1 fusion vector. Five combinations were set up in the following way: BD-ClOr1 + AD-ClPSY1, BD-ClOr1 + AD, BD + AD-ClPSY1, BD-53 + AD-T, and BD-Lam + AD-T. The five combinations were transformed into yeast strain AH109 (Coolaber, Beijing, China). Each combination was cultured on SD/-Leu/-Trp (SD/-LW) medium at 29 °C for 2 d, which was then transferred and streaked onto SD/-Leu/-Trp/-Ade/-His (SD/-LWAH) medium containing 20 mg/L X-α-gal at 29 °C for 2–3 d to test for protein interactions. The primers used are shown in Supplementary Table S2.

For the BiFC assay, *ClOr1* CDS was constructed into the vector pCAMBIA1300-35S-YC155 (YC), and the *ClPSY1* CDS was constructed into the pCAMBIA1300-35S-NY173 (NY) vector, respectively. Then, Agrobacterium strain (GV3101) carrying the binary constructs was transformed together into leaves of five-week-old plants of *N. benthamiana*. After 72 h, the fluorescence was observed under a confocal microscope as described previously[32]. The information of the primers used is shown in Supplementary Table S2.

RNA extraction and gene expression analysis

Total RNA was extracted using the MolPure® Plant RNA Kit (Yeasen, Shanghai, China). Total RNA was reverse transcribed into

cDNA using the PrimeScript™ RT reagent Kit with gDNA Eraser (Takara, Shiga, Japan). To explore the expression patterns of the *ClOr1*, *ClOr2*, and *ClPSY1* genes in the various tissues and flesh of red-fleshed and white-fleshed watermelons at different developmental stages, qRT-PCR analysis was conducted using the Hieff® qPCR SYBR® Green Master Mix from Yeasen (Shanghai, China), and relative expression of the genes was determined by the $2^{-\Delta\Delta C_T}$ method using a relative quantitative method. There were three biological replicates for each tissue and three mechanical replicates for each biological replicate. Gene-specific primers are listed in Supplementary Table S2, and the *ClYLS8* gene was used as the internal reference gene[33]. For transcriptomic analysis, RNA-Seq data of the W1-60 and LSW-177 (SRX2037303) were utilized to further analyze the expression patterns of *ClOr1* and *ClOr2* genes, respectively. All experimental data were statistically analyzed using SPSS 22 and Origin 2024.

Results

Comparison of carotenoid accumulation and developmental patterns of chromoplast in red- and white-fleshed watermelons

After analysis of carotenoid metabolism, a total of 17 carotenoids were detected in two watermelons, such as lycopene, (E/Z)-phytoene, β-carotene, and lutein, and the standard curves of MRM ion-pair information and relative carotenoid content are shown in Supplementary Tables S3, S4, respectively. In the results of the principal component analysis of carotenoids (Fig. 1a), the sum of PC1 and PC2 was 87.13%. The cluster analysis revealed that the 17 types of carotenoid contents varied among watermelons of different flesh colors. In red-fleshed watermelon of the LSW-177, the content of violaxanthin decreased as the fruit developed, while the content of lycopene, β-carotene, β-cryptoxanthin, γ-carotene, α-carotene, lutein, and others generally increased during fruit development. Moreover, lycopene accumulated rapidly at the early developmental stage of red-fleshed watermelon, and its content accounted for 84.8% of the total carotenoid content, and at the ripening period, lycopene, (E/Z)-phytoene, and β-carotene were the major carotenoid constituents, and the sum of the three contents accounted for 94.2% of the total carotenoids (Fig. 1b, c, Supplemental Table S5). In white-fleshed watermelon of W1-60, the content of violaxanthin, neoxanthin, capsorubin, zeaxanthin, and lutein decreased with fruit development, while the content of canthaxanthin increased with fruit development. During the development of white-fleshed watermelon, lutein was the main carotenoid component. The lutein content of 18 and 34 DAP accounted for 76.6% and 67.5% of the total carotenoids, respectively (Fig. 1b, c, Supplemental Table S5).

Different patterns were found in the microscopic and submicroscopic structures of the LSW-177 and W1-60 watermelon fruits after observation. There was no visible pigment accumulation in the longitudinal section of 10 DAP fruits of two watermelons (Fig. 2a1, d1), and no chromoplast was in the flesh cells (Fig. 2b1, e1),

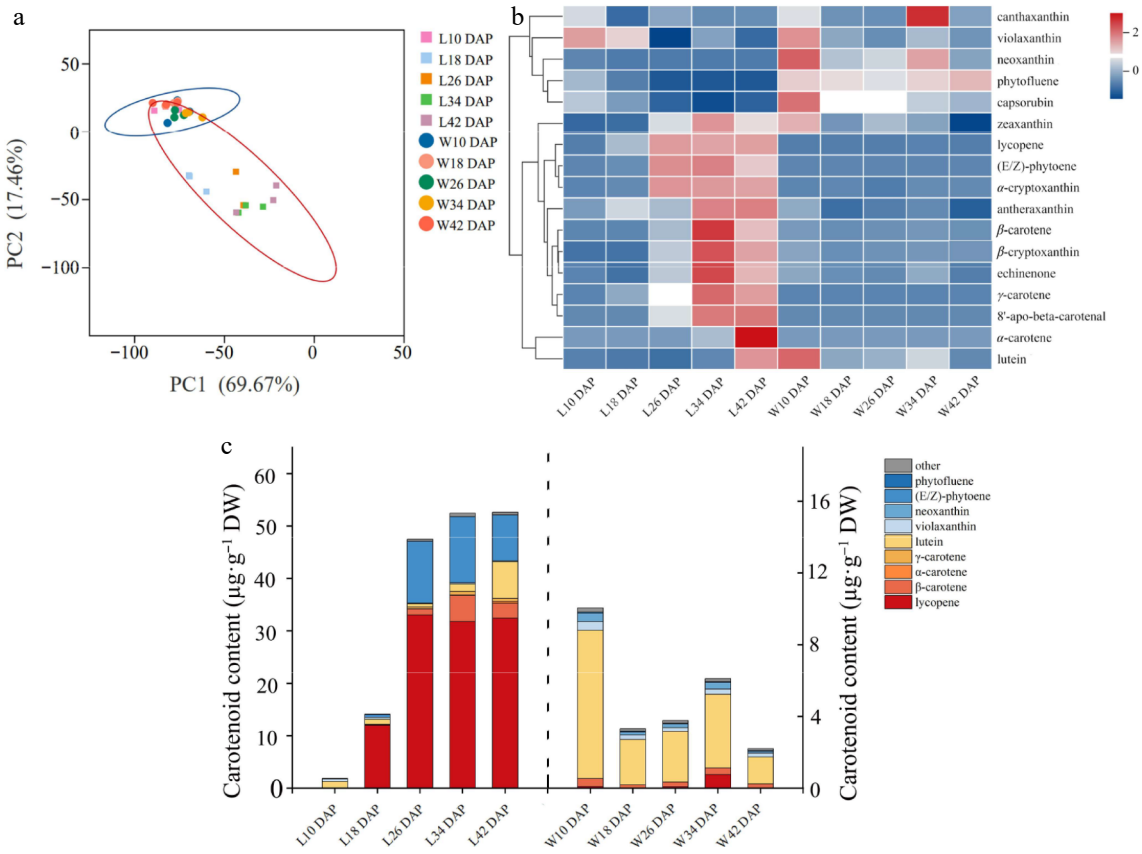

Fig. 1 Carotenoid accumulation and developmental patterns of chromoplast in red- and white-fleshed watermelons. (a) Main component analysis of carotene. The cube with five colors indicates the flesh of LSW-177 at 10, 18, 26, 34, and 42 d after pollination, covered by a red oval. The five colored circles indicate the flesh of W1-60 at 10, 18, 26, 34, and 42 d after pollination, covered by a blue oval. The data was processed $\log_2$ (N). (b) Cluster analysis of carotene: the data have been standardized by Z-score processing. (c) Carotenoid composition analysis: the content of carotenoid in fruit of L10, L18, L26, L34, and L42 DAP is shown on the left Y axis, and the content of carotenoid in fruit of W10, W18, W26, W34, and W42 DAP is shown on the right Y axis.

but the red-fleshed watermelon contained more proplastid (Fig. 2c1, f1). In the longitudinal section of 18 DAP fruits of red-fleshed watermelon, carotenoids were deposited around the seeds (Fig. 2a2), globular chromoplasts appeared in the cells, and some chromoplasts formed endogenous plastoglobules (Fig. 2b2, c2), while the white-fleshed watermelon 18 DAP flesh was still white (Fig. 2d2, e2, f2). The 26 DAP flesh of red-fleshed watermelon was uniformly colored (Fig. 2a3) with lots of red carotenoid crystals and more plastoglobules (Fig. 2b3, c3), while the 26 DAP flesh of white-fleshed watermelon had globular chromoplasts appearing in the cells with fewer plastoglobules (Fig. 2d3, e3, f3). From 34 to 42 DAP in red-fleshed watermelon, flesh color gradually continued to deep red, more carotenoid crystals were accumulated in the cells, the membrane structure of the chromoplast gradually disappeared, and plastoglobules were dispersed into the cytoplasm (Fig. 2a4, a5, b4, b5, c4, c5). In white-fleshed watermelon, there was a

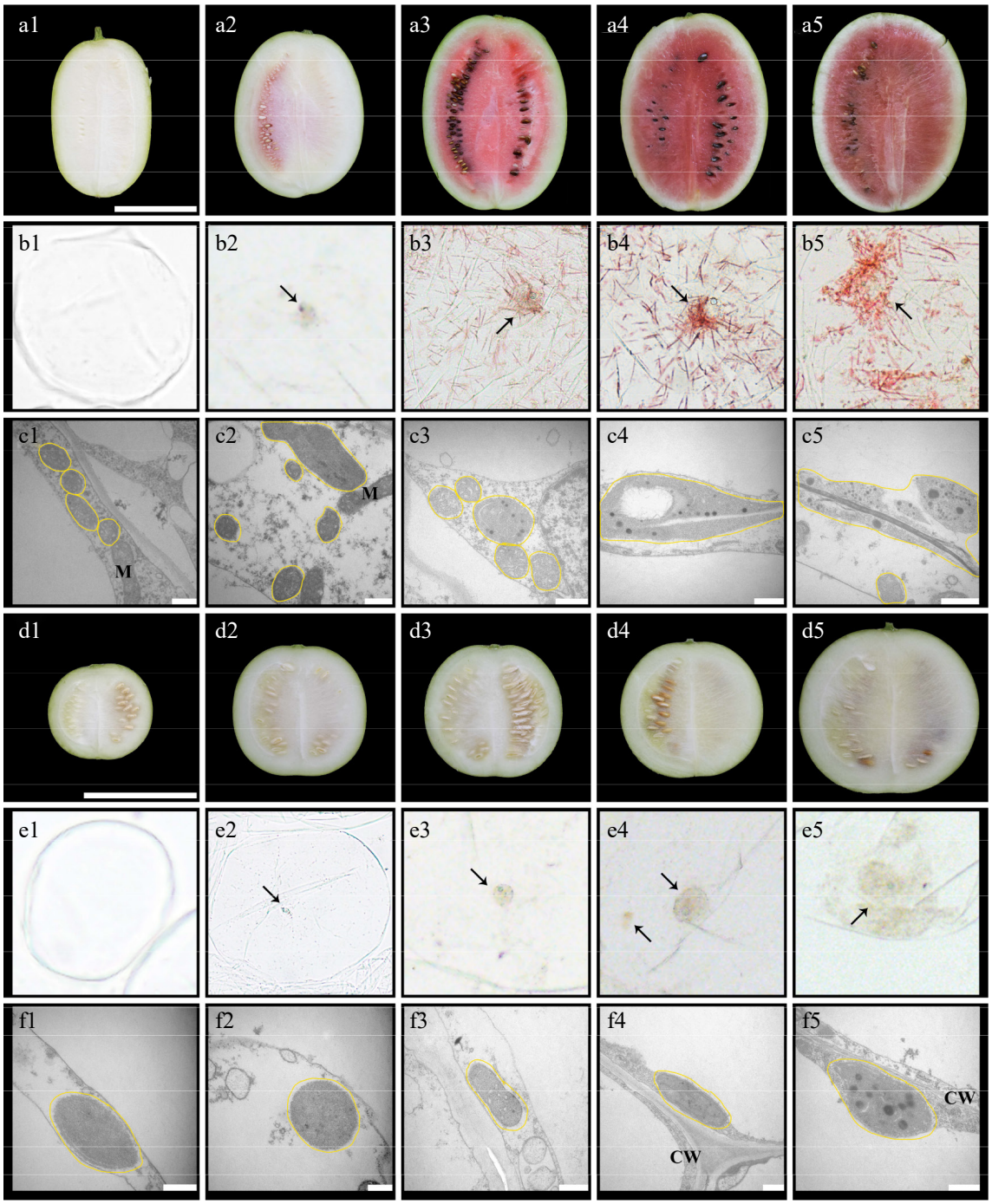

Fig. 2 Cytological observation of chromoplast in the flesh of watermelons (LSW-177 and W1-60). The letters (a)–(c) are the longitudinal section, cell microstructure, and cell sub-microstructure of the fruit of LSW-177, respectively; the letters (d)–(f) are the longitudinal section, cell microstructure, and cell sub-microstructure of the fruit of W1-60, respectively. The scale of (a) and (d) is 10 cm, and the scale of (c) and (f) is 0.5 μm. The numbers (1), (2), (3), (4), and (5) after the letters represent 10, 18, 26, 34, and 42 DAP, respectively. The black arrow points to the chromoplast, the yellow line represents the plast. M: mitochondria; CW: cell wall.

pale yellow pigmentation around the seeds, and the number of chromoplasts and plastoglobules increased (Fig. 2d4, d5, e4, e5, f4, f5).

Identification of key *Or* genes regulating carotenoid accumulation in watermelon fruit

To identify the key *Or* genes regulating carotenoid accumulation in watermelon fruit, the amino acid sequence of the *AtOr* gene in Arabidopsis was used as the reference sequence for pairwise comparison and screening in the protein database of watermelon genome (97103), and the *Cla97C01G005050* and *Cla97C04G076970* genes were identified as members of the *Or* gene family in watermelon genome and named the *ClOr1* and *ClOr2* genes, respectively. The *ClOr1* gene is located on chromosome 1, with a total length of 6,621 bp, and the *ClOr2* gene is located on chromosome 4, with a

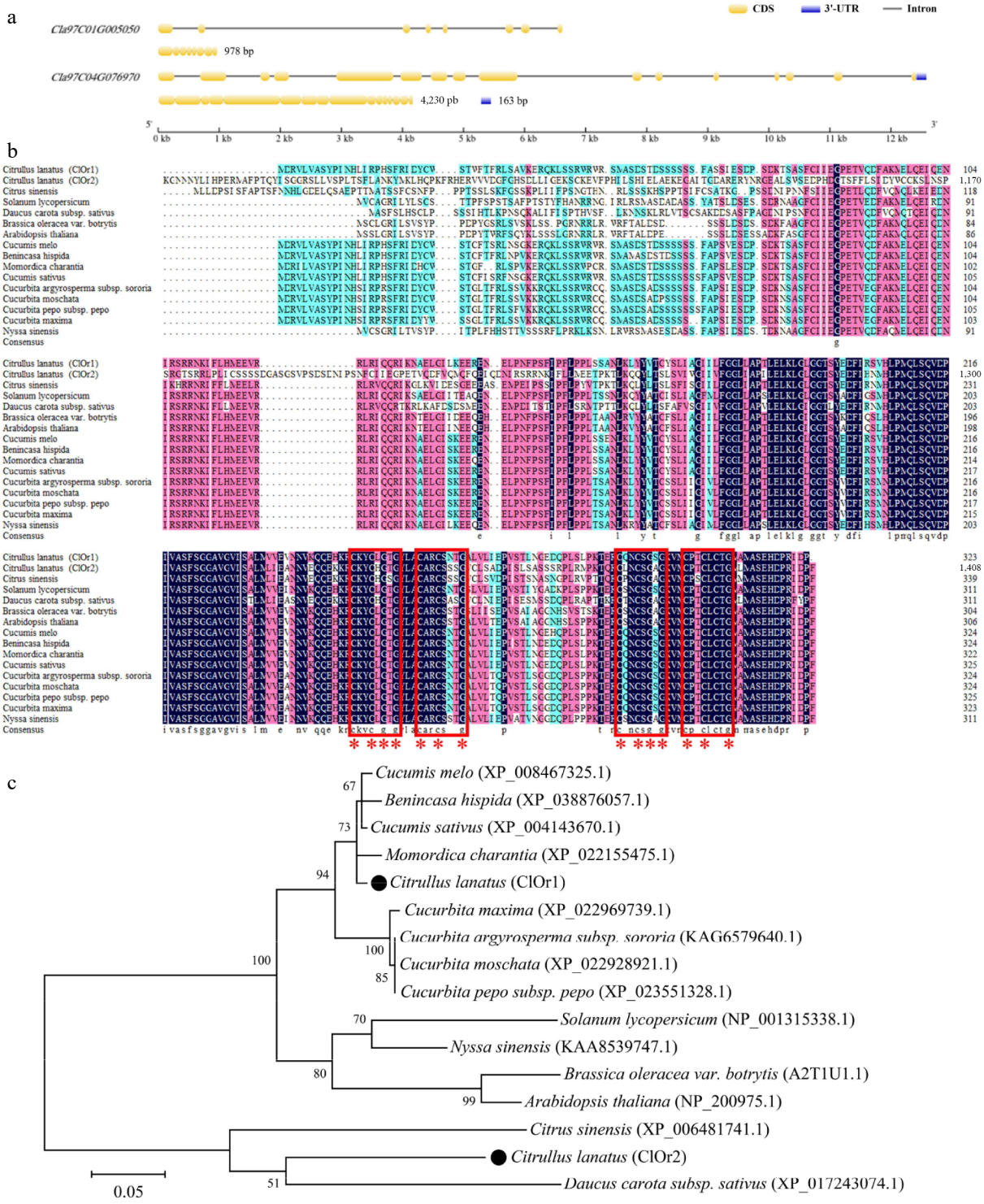

Fig. 3 Sequence alignment and phylogenetic analysis of ClOr. (a) Structure of the *ClOr1* and *ClOr2* genes. (b) Sequence analysis of the Or protein. The red box marks two (CxxCxGxG) motifs and two (CxxCxxxG) motifs, and the red '*' marks eight cysteine and six glycine residues that are highly conserved. (c) Phylogenetic tree of the Or protein. The bar indicates an evolutionary distance of 0.05%.

total length of 12,579 bp (Supplementary Table S6). The structures of the *ClOr1* and *ClOr2* genes analyzed by the CSDS (v2.0) (Fig. 3a), the *ClOr1* gene contains eight exons and seven introns, and the *ClOr2* gene contains 16 exons and 15 introns; their full-length CDS were 978 bp and 4,230 bp, respectively. The protein sequences of ClOr1 and ClOr2 harbor the cysteine-rich DnaJ and HSP40 zinc-finger structural domains (two CxxCxGxG motifs and two CxxCxxxG motifs) in the multiple sequence comparison and conserved structural domain analysis (Fig. 3b). In the phylogenetic tree (Fig. 3c), the *Or* genes were mainly divided into two clusters. the ClOr1 was closest to bitter gourd (XP_022155475.1), cucumber (XP_004143670.1), winter melon (XP_038876057.1), and melon (XP_008467325.1). The ClOr2 was clustered into a clade with carrot (XP_017243074.1) and sweet orange (XP_006481741.1).

The expression levels of the *ClOr1* and *ClOr2* genes were increasing in the flesh of red- and white-fleshed watermelons during fruit development (Fig. 4a), with expression peaking at 34 DAP. Moreover, the expression level of *ClOr1* in the flesh of red-fleshed watermelon was higher than that in white-fleshed watermelon at the same developmental stage. However, there was no significant difference in the expression level of *ClOr2* between the flesh of red- and white-fleshed watermelons. Furthermore, the expression profiles of the *ClOr1* and *ClOr2* genes were examined in various tissues of red- and white-fleshed watermelons at 34 DAP. The *ClOr1* gene was most highly expressed in the flesh of red-fleshed watermelon and the leaves of white-fleshed watermelon; however, the *ClOr2* gene exhibited the highest expression in the female flower of red-fleshed watermelon and in the male flower of white-fleshed watermelon. Notably, compared to *ClOr2*, *ClOr1* could play a more important role in the red flesh of watermelon based on the above expression level analysis.

In the correlation analysis between *ClOr* gene expression and carotenoid content (Fig. 4b), the expression levels of the *ClOr1* gene in the flesh of red-fleshed watermelon (LSW-177) and white-fleshed watermelon (W1-60) were significantly correlated with the total carotenoid content at different developmental stages; the correlation coefficients were 0.96 (relative expression and total carotenoid content) and 0.93 (FPKM and total carotenoid content), while the correlation coefficients of the *ClOr2* gene were 0.23 and 0.87, respectively. The obtained results suggest that the *ClOr1* gene had a higher correlation with carotenoid content in the flesh of watermelon at different developmental periods than that of the *ClOr2* gene. Therefore, it is speculated that the *ClOr1* gene was involved in carotenoid biosynthesis in watermelon flesh.

Cloning and sequence analysis of *ClOr1*

After cloning the *ClOr1* gene successfully (Supplementary Fig. S1a, S1b), the full-length CDS of the *ClOr1* gene was 978 bp in red- and white-fleshed watermelons, encoding 325 amino acids. The 87th base of the *ClOr1* gene cloned from the flesh of red-fleshed watermelon (LSW-177) was G, encoding the 29th amino acid, tryptophan (Trp), which was the same as that of Watermelon (97103) v2.5 Genome, while the 87th base of the *ClOr1* gene cloned from the flesh of white-fleshed watermelon (W1-60) was T, which encodes a cysteine (Cys) here. A dCAPS marker was designed to distinguish the *ClOr1* gene in the LSW-177 and W1-60. PCR and restriction enzyme digestion were used to distinguish between G/G, T/T, and G/T. The results confirmed the SNP variation could play an important role in distinguishing the red- and white-fleshed watermelon (Supplementary Fig. S1c, S1d). Secondary and tertiary structure prediction of ClOr1^{Trp} and ClOr1^{Cys} proteins (Supplementary Fig. S2) showed: ClOr1^{Trp} protein consisted of 26.32% α-helix, 10.84% extended strand, 1.24% β-turn, and 61.61% random coil; ClOr1^{Cys} protein consisted of 23.53% α-helix, 9.91% extended strand, 0.93% β-turn, and 65.63% random coil. According to the suggestion, the protein stability could be changed by their structural difference; proteins with a higher proportion of α-helix structure exhibited greater stability. Therefore, the SNP (Cys/Trp) caused a change in ClOr1 protein stability; the stability of ClOr1^{Trp} protein was higher than that of ClOr1^{Cys} protein.

SNP genotype analysis in the *ClOr1* gene of watermelon germplasm resources

The non-single nucleotide from guanine (G/G) in the LSW-177 to thymine (T/T) in the W1-60 may not only change the gene sequence, but also change the protein sequence of ClOr1 (Fig. 5a). To further confirm whether the SNP (87 bp, T/G, and Cys/Trp) in the *ClOr1* gene

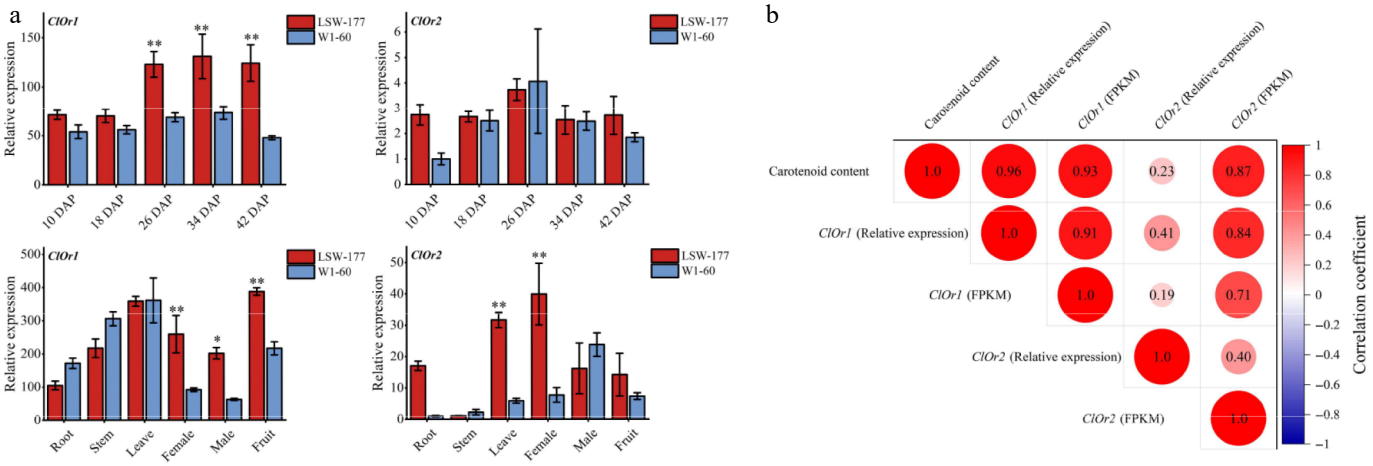

Fig. 4 Expression analysis of the *ClOr* gene in watermelons. (a) Expression analysis of the *ClOr* gene in red- and white-fleshed watermelon. Each data point represents the mean of three biological replicates, the error bar represents the mean ± standard error value, * significant difference, $p < 0.05$; ** $p < 0.01$ (two-tailed). (b) Correlation analysis between the *ClOr* gene expression and carotenoid content. Relative expression refers to the fluorescence quantitative data of the *ClOr* gene in LSW-177 and W1-60 materials at different developmental stages, and FPKM refers to the RNA-Seq data of the *ClOr* gene in LSW-177 (PRJNA338036) and W1-60 at different developmental stages. The number in the circle pattern is the Pearson correlation coefficient (two-tailed), respectively.

affects the flesh color of watermelon, the genomic data of 414 publicly available watermelon germplasm resources provided by Guo et al[34], together with 14 germplasm resources of watermelon saved in the laboratory, were utilized to analyze the genotypes of this SNP in the *ClOr1* gene. Further, integrating the genotyping and phenotyping results among these 428 watermelon germplasm resources (Supplementary Table S7) showed that, 188 out of 197 red-fleshed watermelons had the G/G genotype, 17 out of 18 pink-fleshed watermelons had the G/G genotype, and 15 out of 16 orange-fleshed watermelons and 20 out of 21 yellow-fleshed watermelons had the G/G genotype, respectively. In contrast, 14 out of 18 pale yellow-fleshed watermelons and 34 out of 49 white-fleshed watermelons had the T/T genotype (Supplementary Table S8, Fig. 5b); these results suggested that this SNP variant in 428 watermelon germplasm resources plays a significant role in controlling the flesh color of watermelons.

Moreover, because the LSW-177 belongs to *C. lanatus,* ssp. *vulgaris* and the W1-60 belongs to *C. amarus*, the geographic origin

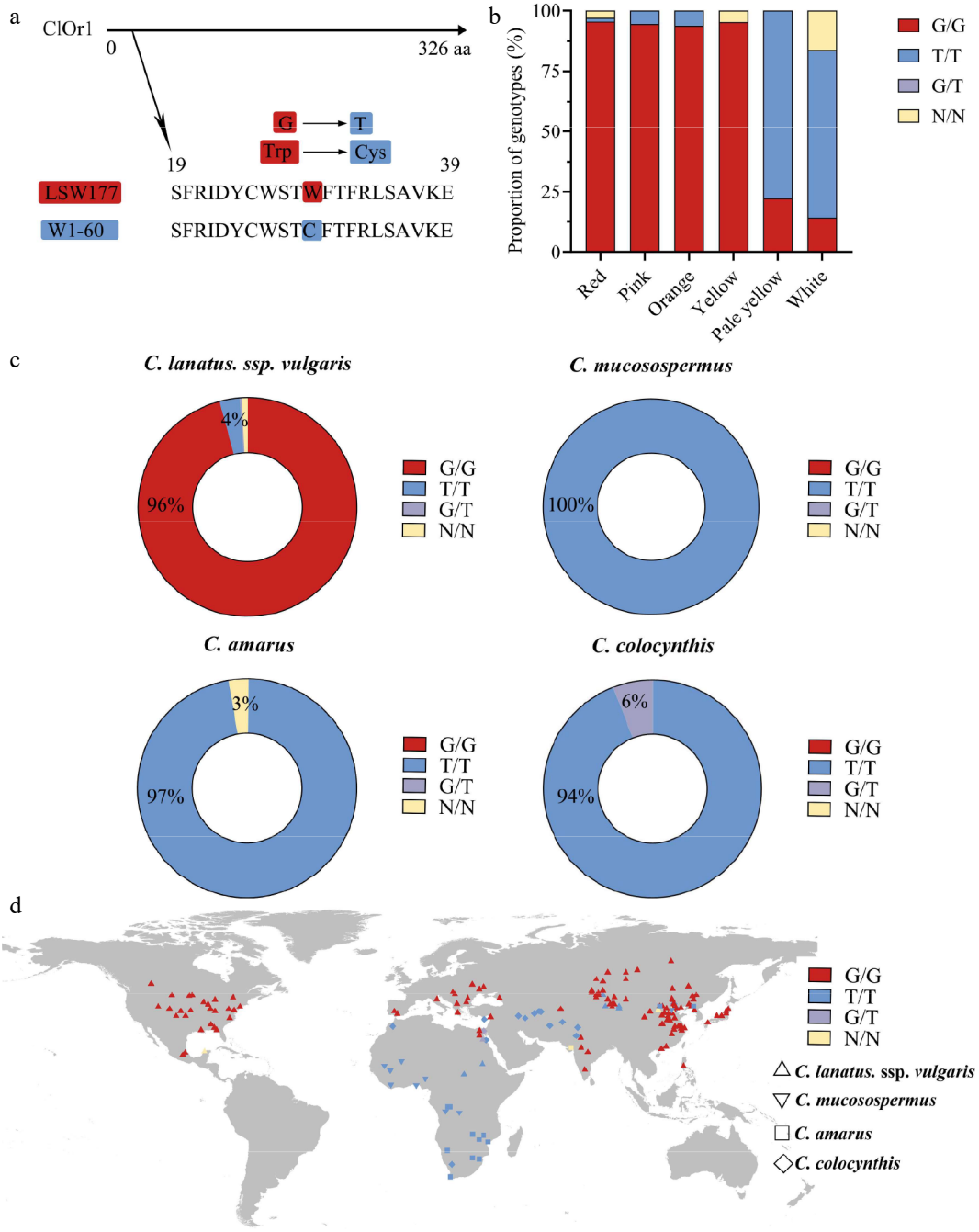

Fig. 5 A single SNP variation in the *ClOr1* gene can affect the formation of watermelon flesh color. (a) Sequence variation of ClOr1 protein between LSW-177 and W1-60. A non-synonymous mutation from guanine (G) to thymine (T) at the 29th amino acid of ClOr1 resulted in an amino acid variation from tryptophan (Trp) to cysteine (Cys). (b) Genotype proportions of watermelons with different flesh colors (red, pink, orange, yellow, pale yellow, white). The red sections represented the G/G genotype identical to LSW-177, the blue sections represented the T/T genotype identical to W1-60, the purple sections represented the G/T genotype, and the orange sections represented unknown. (c) Genotype of 406 watermelon accessions using a doughnut chart. (d) Geographical distribution of genomic variations in the *ClOr1* gene of 428 watermelon accessions. *C. lanatus,* ssp. *vulgaris* was represented by an upright triangle, *C. mucosospermus* was represented by an inverted triangle, *C. amarus* was represented by a square, and *C. colocynthis* was represented by a rhombus.

of 428 watermelon germplasm resources were also re-analyzed for insight into the function of the *ClOr1* gene. The results showed that there were 341 *C. lanatus*, ssp. *vulgaris* accessions, 96% of which were G/G genotypes; 13 *C. mucosospermus* accessions, all of which were T/T genotypes; 97% of 34 *C. amarus*; and 94% of 17 *C. colocynthis* accessions were T/T genotypes (Fig. 5c). G/G genotypes are mainly found in humid and rainy East Asia, North America, and the Mediterranean region, while T/T genotypes are mainly found in arid Africa and West Asia (Fig. 5d). The high concordance between genotypes and ecotypes indicated that this SNP could well distinguish white-fleshed watermelon from non-white-fleshed watermelon, and combined with the expression level of the *ClOr1* gene, it was significantly and positively correlated with total carotenoid content (Fig. 4). These results further suggested that the *ClOr1* gene might be a key gene affecting the flesh color formation in watermelon.

Subcellular localization of ClOr1 protein

The results of subcellular localization of ClOr1 protein exhibited that the green fluorescence expressed by the pBWA(V)HS-Osgfp-ClOr1 fusion vector completely overlapped with the red fluorescence of the cell nucleus Marker (ClOr1-GFP), which significantly indicated that the ClOr1 protein was expressed in the nucleus (Supplementary Fig. S3). Meanwhile, the pBWA(V)HS-Osgfp empty vector and cytosolic Marker showed normal green fluorescence and red fluorescence (Free-GFP), respectively, indicating that the fluorescent proteins of both BWA(V)HS-Osgfp and cytosolic Marker could be expressed normally, which depicted that the experimental results were highly credible.

Total carotenoid content in OE-ClOr1 tomato fruits at different developmental stages

To elucidate the role of the *ClOr1* gene in carotenoid accumulation, tomato plants with *ClOr1* overexpression were generated. The positive transgenic tomato plants (OE-1, OE-2, OE-3) flowered earlier than the WT tomato (Fig. 6a), and the fruits ripened earlier than the WT tomato (Fig. 6b). The fruits of OE tomato were at the mature green stage for 31 ± 1 DPA; the breaker stage and red ripe stage were at 34 ± 2 DPA and 36 ± 2 DPA respectively (DPA: Days post anthesis); while WT tomato fruits reached the mature green and breaker stages at 36 ± 3 DPA and 40 ± 5 DPA, respectively (Fig. 6c).

After statistical analysis, OE tomato took significantly less time than WT tomato from sowing to anthesis (S to A) and fruit breaker to red (B to R) (Fig. 6d), which showed that overexpression of the *ClOr1* gene in tomato can promote flowering and ripening. Compared with the WT tomato, the expression level of the *ClOr1* gene was significantly increased in OE tomato fruits at different developmental stages, ranging from 91.4 to 440.1-fold, and reached a peak at the red ripe stage of tomato (36 DPA) (Fig. 6e). Meanwhile, the total carotenoid content in the fruits of OE tomatoes at different developmental stages was significantly increased compared to WT tomatoes (Fig. 6f), with the increase ranging from 1.8 to 19.2-fold. In addition, the correlation analysis showed that the gene expression of *ClOr1* in the fruits of OE tomatoes was significantly and positively correlated with the total carotenoid content (Fig. 6g).

TRV-mediated *ClOr1* gene silencing decreased carotenoid accumulation in the watermelon fruit flesh

Significant phenotypic changes were observed in watermelon fruits after TRV-mediated *ClOr1* gene silencing. It was found that the pTRV2-injected fruit portion was normally transformed to red, whereas the pTRV2-ClOr1-silenced fruit could not be smoothly transformed to red (Fig. 7a). In the qRT-PCR analysis and carotenoid content assay (Fig. 7b), compared to the control group pTRV2, the expression level of the *ClOr1* gene was down-regulated by 23.6%, and the total carotenoid content was significantly down-regulated in the experimental group pTRV2-ClOr1. The results contributed to the fact that silencing the *ClOr1* gene resulted in a significant reduction of total carotenoid content in watermelon fruit flesh.

The interaction between ClOr1 and ClPSY1 prompted the synthesis and accumulation of carotenoids in watermelon flesh

The Y2H assay was used to identify the interaction between ClPSY1 and ClOr1; the ClOr1 and ClPSY1 were constructed into the DNA-binding domain (BD) and the transcription activation domain (AD) of the GAL4 system, respectively. Compared to the control group, only yeast cells harboring AD-ClOr1 + BD-ClPSY1 grew normally and exhibited blue coloration on SD/-Leu/-Trp/-Ade/-His medium containing 20 mg/L X-α-gal, confirming a strong interaction between ClOr1 and ClPSY1 (Fig. 8a). Higher α-GAL activity than other groups also revealed a strong interaction between ClOr1 and ClPSY1 proteins (Fig. 8b). To verify whether ClOr1 and ClPSY1 interact *in vivo*, bimolecular fluorescence complementation (BiFC) assays were performed. YC-ClOr1 + NY-ClPSY1 showed a strong yellow fluorescence signal in the YFP fluorescence channel that was much higher than the background, and the yellow fluorescence overlapped with the spontaneous fluorescence of chloroplasts. These results indicated that the ClOr1 protein and ClPSY1 protein exhibited direct interaction in tobacco leaf epidermal cells, and their interaction is located in the chloroplast (Fig. 8c).

Then, it was found that the expression level of the *ClPSY1* gene in the LSW-177 material gradually increased with fruit development and reached its peak at 26 DAP. Except for 10 DAP, the expression levels at all other stages were significantly higher than those in W1-60 (Fig. 8d). The expression level of the *SlPSY1* gene rose sharply during the mature green stage (31 DPA) of transgenic tomato fruit and peaked at the red ripe stage (36 DPA), proving that the upregulation of the *ClOr1* gene expression level can promote the increase in the *SlPSY1* gene expression level (Fig. 8e). In VIGS, the expression level of the *ClPSY1* gene decreased significantly, indicating that the downregulation of the *ClOr1* expression level can inhibit the expression of the *ClPSY1* gene (Fig. 8f). Correlation analysis showed that the expression of *ClPSY1* and *SlPSY1* genes was significantly correlated with the expression of the *ClOr1* gene and the total carotenoid content (Supplementary Fig. S4a, S4b).

Discussion

The flesh color of watermelon is an important trait closely associated with nutritional and economic value. The reason for the different flesh colors of watermelon is the difference in the composition and accumulation of carotenoid content[35]. In this study, the results of carotenoid detection at different stages of development in the flesh of red-fleshed watermelon (LSW-177) and white-fleshed watermelon (W1-60) indicated that mature fruit flesh of the LSW-177 primarily contained lycopene, (E/Z)-phytoene, and β-carotene, while the primary carotenoid in W1-60 fruit flesh was lutein (Fig. 1, Supplementary Tables S3, S4, S5). It has been reported that red-fleshed watermelons contained high levels of lycopene, yellow-fleshed watermelons contained traces of lutein and β-carotene or a small

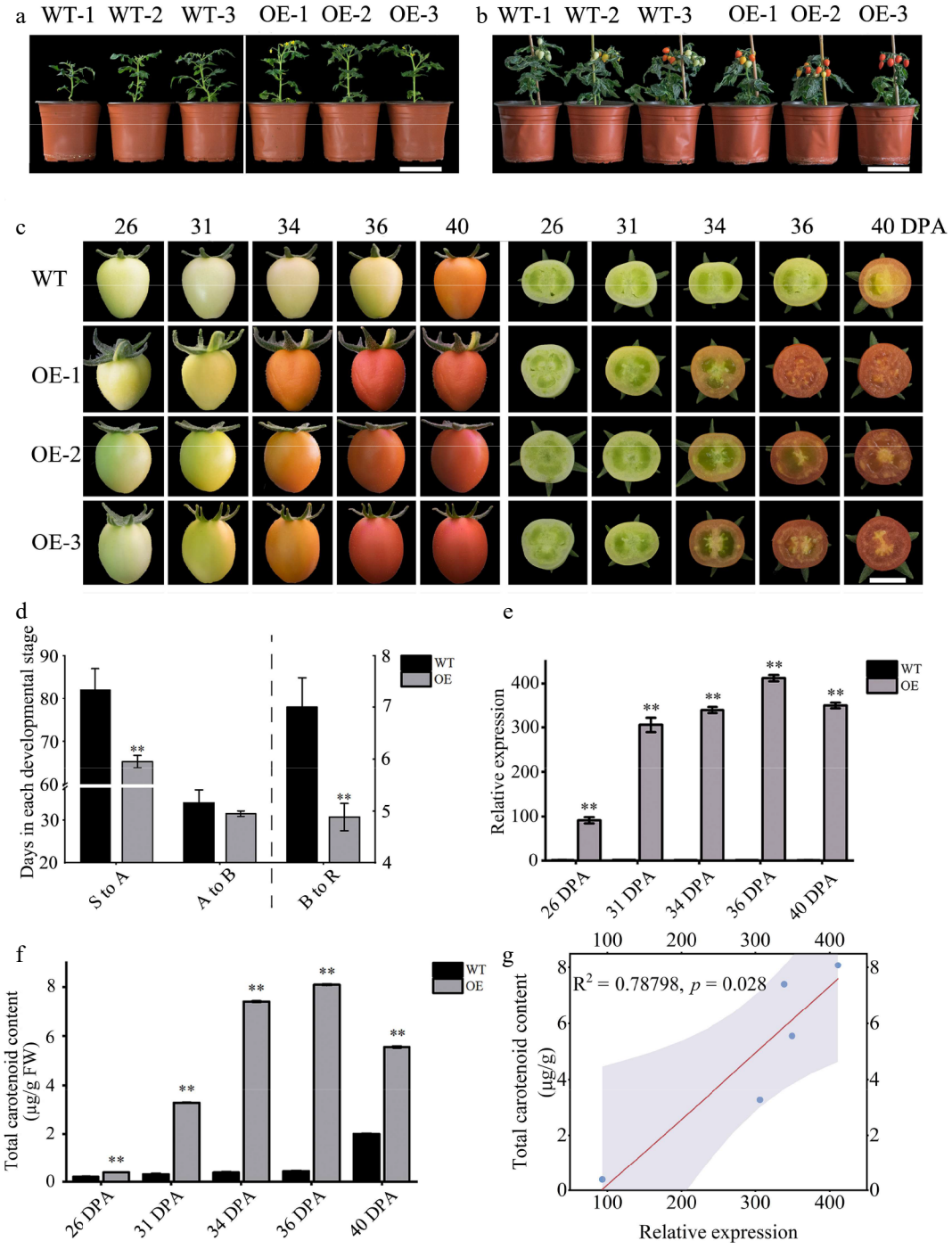

Fig. 6 Phenotypic and gene expression analysis of WT and OE tomatoes. (a) First flowering state of tomato plants, scale = 10 cm. (b) Fruit development status of tomato plants, scale = 10 cm. (c) Tomato fruit phenotype, scale = 1 cm. (d) Number of days required for each developmental period in tomato fruit; see the left Y axis for (S to A) and (A to B), and the right Y axes for (B to R). (e) The expression level of the *ClOr1* gene in fruits at different ripening stages, in which the expression level of the 26 DPA fruit of WT tomato was used for calibration. (f) Total carotenoid content in fruits at different ripening stages. In (d)–(f), each data point represents the mean of three biological replicates, the error bar represents the mean ± standard error value, ** significant difference between the WT and OE tomatoes, $p < 0.01$ (two-tailed). (g) Correlation analysis between the *ClOr1* gene expression and total carotenoid content.

amount of pre-lycopene, and orange-fleshed watermelons contained orange pre-lycopene and β-carotene[36,37]. The white-fleshed watermelon variety (ZXG507) contained only small amounts of lutein and violaxanthin[38]. This study further verified that the composition and amount of carotenoid content in watermelons affected the formation of flesh color.

Chromoplast is the key organelle for carotenoid biosynthesis and accumulation[39]. The interior of chromoplasts produces carotenoid-lipoprotein substructures to sequester and stably store large amounts of carotenoids[40]. The results of chromoplast observation in the fruit of red-fleshed watermelon (LSW-177) and white-fleshed watermelons (W1-60) at different developmental stages showed

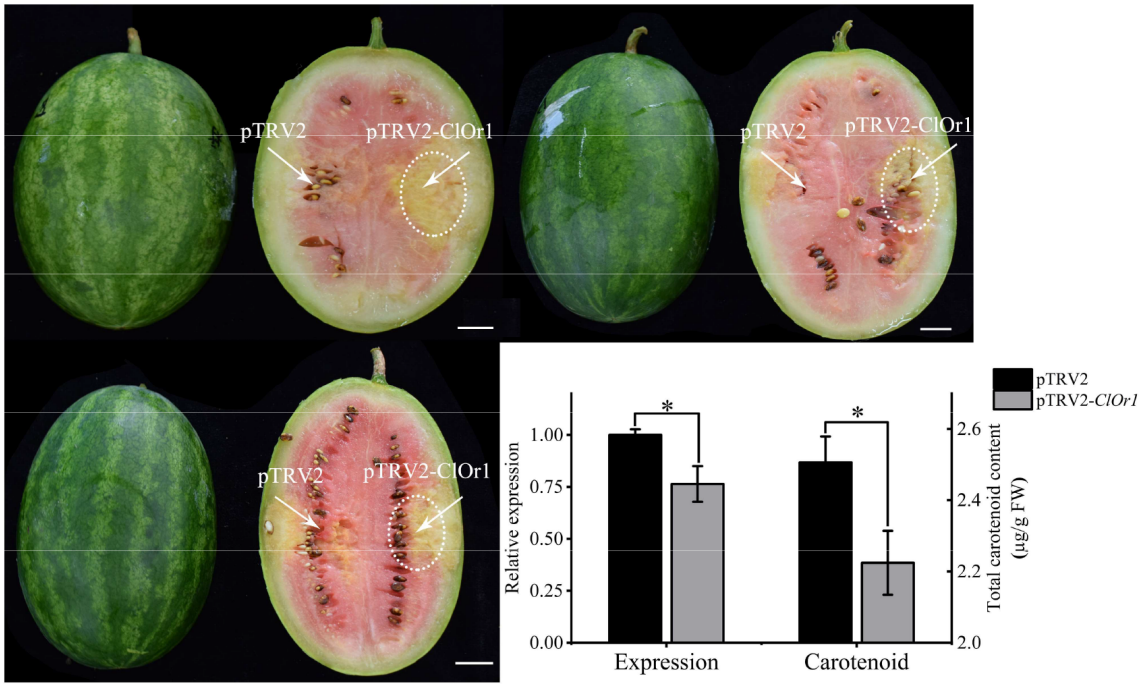

Fig. 7 Analysis of watermelon flesh transformation effect. (a) VIGS effect diagram of watermelon flesh, scale = 2 cm. (b) qRT-PCR analysis and total carotenoid detection, and the expression level of pTRV2 in the control group was used for calibration. * Significant difference between pTRV2 of the control group, and pTRV2-ClOr1 of the experimental group, $p < 0.05$ (two-tailed). Each data point represents the mean of three biological repeats, and the error bar represents the mean ± standard error value.

that the LSW-177 was rich in carotenoid crystals, and the number and size of plastids also continued to increase, while the fruits of W1-60 contained only globular chromoplasts and developed slowly (Fig. 2). The crystalline chromoplasts formed in the mature fruit cells of red-fleshed watermelons were related to the accumulation of lycopene and β-carotene, while the only globular chromoplasts in the fruit cells of white-fleshed watermelons were related to the accumulation of carotenoids such as lutein. The compositions and contents of carotenoids can affect the differentiation of chromoplast, which has been reported in red-fleshed watermelon, red tomato, and red-fleshed papaya[19,41,42]. In studies of colorless or weakly colored tissues such as young watermelon fruit[19], citrus fruit[43], white carrot root system[44], white potato tuber[45], and flower bulb[20], the chromoplasts could be transformed from proplastids. Therefore, it is hypothesized that the chromoplasts in the fruit cells of red- and white-fleshed watermelon are transformed from proplastids.

It is well established that the *Or* gene can indirectly regulate plant carotenoid accumulation by regulating attributes such as differentiation, number, and size of chromoplasts[7,46]. The function of acquired mutations in the *Or* gene has been shown to be related to the regulation of the differentiation of chromoplasts to promote carotenoid accumulation in studies of the cauliflower *BoOr* natural mutant[20], the melon *CmOr* natural mutant[21], and the Arabidopsis thaliana *AtOr*^{His} gene[47]. Two genes of the Or family in watermelons were characterized, *ClOr1* and *ClOr2* (Fig. 3, Supplementary Table S6). The expression of *ClOr1* and *ClOr2* in the fruit at different developmental stages and 34 DAP root, stem, leaf, and female and male flower tissues of LSW-177 and W1-60 watermelons was determined, and it was found that the expression level of the *ClOr1* gene was higher in the mature fruit of red-fleshed watermelons than in other tissues. The expression level of the *ClOr1* gene was higher in all tissues of watermelon compared with that of the *ClOr2* gene, and at the same time, the expression of the *ClOr1* gene was significantly correlated with the carotenoid content of the flesh of red- and white-fleshed watermelons at different developmental stages (Fig. 4). RNA-Seq data from watermelon (97103, v2.5) with different flesh colors were used to further analyze the expression patterns of the *ClOr1* and *ClOr2* genes, and the transcript levels of the *ClOr1* genes in red-, pink-, yellow-, and white-fleshed watermelons increased with fruit maturity, but the *ClOr2* gene did not show any significant changes[6,48,49]. A single-base missense mutation SNP (87 bp, T/G, Cys/Trp) was found in the *ClOr1* gene, after cloning the *ClOr1* gene and comparing the sequences of the LSW-177 and W1-60 (Supplementary Fig. S1). A dCAPS tool was developed based on this SNP and combined with 428 germplasm resources of watermelon. It was confirmed that the SNP in the *ClOr1* gene could well discriminate between white-fleshed watermelon germplasm resources and non-white-fleshed watermelon germplasm resources (Fig. 5, Supplementary Tables S7, S8), indicating that the *ClOr1*^{Trp} gene could promote carotenoid accumulation in watermelon flesh. Therefore, the *ClOr1*^{Trp} in the watermelon of LSW-177 was identified as a key candidate for promoting carotenoid accumulation in the fruit flesh.

Or has been shown as an important genetic tool for carotenoid enhancement in major plants[17,28]. Overexpression of the *OsOR* gene modified thylakoid development in rice and reduced carotenoid content[50]. Tomato SlOR protein regulated the accumulation of chlorophyll and carotenoid, and affected tomato adaptation to high light intensity and disease resistance[51]. The *Or* gene isolated from a cauliflower mutant increases carotenoid content in potato tubers[52]. The Arabidopsis *Or* gene increased the carotenoid content of endosperm significantly in transgenic rice and maize lines[24,53]. In this study, tomato was transformed with the *ClOr1*, resulting in fruit coloration and much higher carotenoid accumulation in the fruit (Fig. 6). In addition, the down-regulation of the

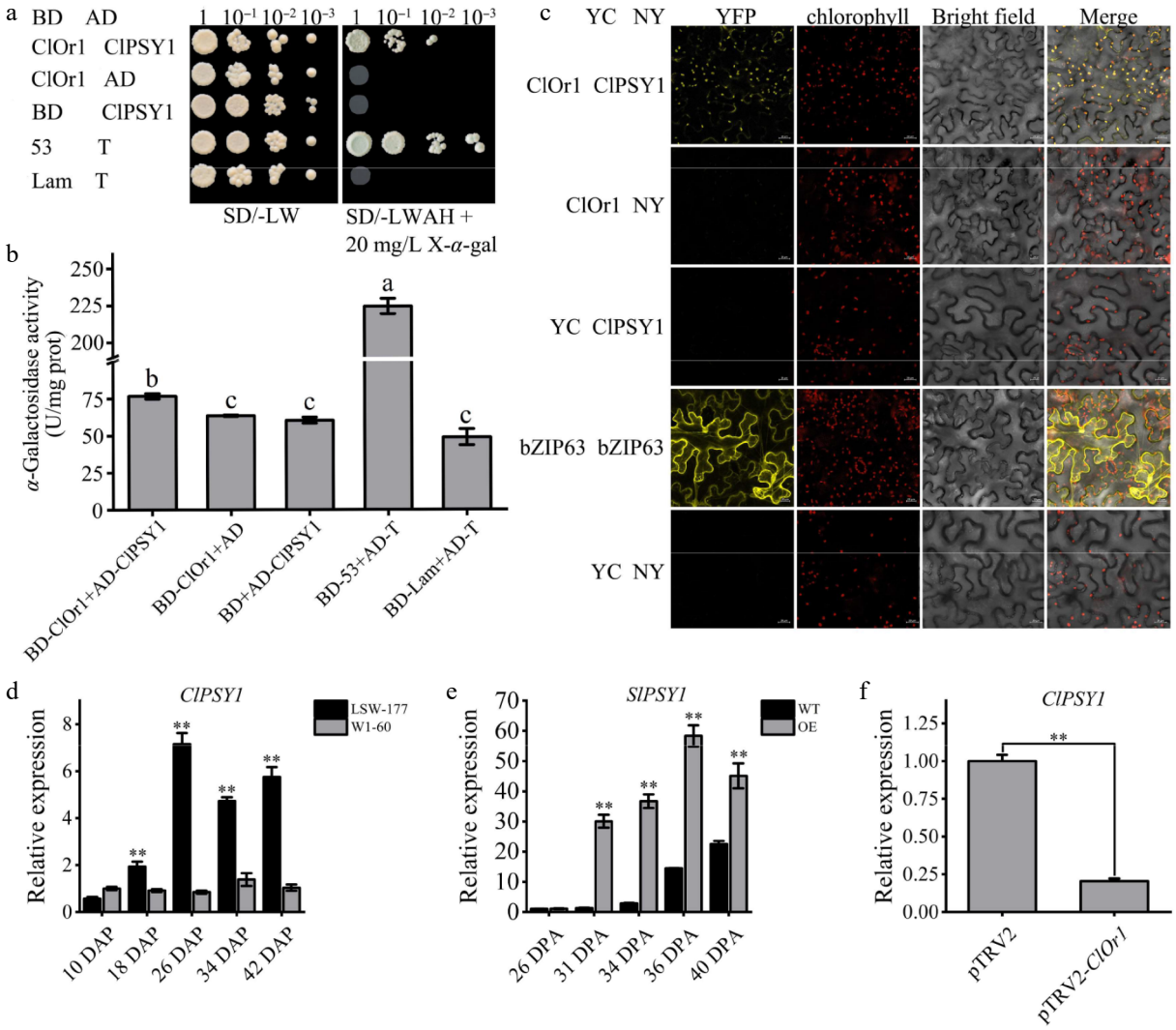

Fig. 8 ClOr1 interacted with ClPSY1. (a) Y2H assays. Growth of co-transformed yeast on non-selective SD/-LW medium and selective SD/-LWAH medium. Positive control BD-53 + AD-T (pGBKT7-53 + pGADT7-T), negative control BD-Lam + AD-T (pGBKT7-Lam + pGADT7-T). (b) α-Galactosidase activity detection. U/mg prot, unit enzyme activity, is 1 nmol p-nitrophenol per mg histone per hour. The results of the one-way analysis of variance were indicated by different lowercase letters ($p < 0.05$). (c) BiFC assays. YFP: yellow fluorescent channels; Bright field: chloroplast spontaneous fluorescent channels; Merge: superposition field. YC-bZIP-63 + NY-bZIP-63 and YC + NY were used as positive control and negative control, respectively. (d), (f) Expression analysis of the *ClPSY1* gene in watermelons. (e) Expression analysis of the *SlPSY1* gene in tomato fruits at different ripening stages. Bar data are the means of three biological replicates ± standard error value, * $p < 0.05$; ** $p < 0.01$ (two-tailed).

expression level of the *ClOr1* gene in the virus-induced *ClOr1* gene silencing assay resulted in a significant down-regulation of carotenoid content (Fig. 7). Thus, the *ClOr1* gene functions to regulate carotenoid accumulation. Most studies have shown that Or proteins interact with phytoene synthase PSY[47,54]. So far, the ClPSY1 has been confirmed to regulate the formation of watermelon flesh color and is a key component of the carotenoid metabolic pathway[55,56]. The results of the Y2H and α-galactosidase activity difference in this study indicated that there was a strong interaction between the ClOr1 protein and the ClPSY1 protein; the results of the BiFC assays indicated that the interaction between the ClOr1 protein and ClPSY1 protein was located in the plastid, while the ClOr1 protein was located in the nucleus. To the best of current knowledge, the subcellular localization of the *Or* gene may be dynamic and change according to the physiological state or developmental stage of the cell. For example, in Arabidopsis, AtOr had a dual localization pattern of nucleus and plastid[57]. Meanwhile, in BoOr transgenic Arabidopsis, the cauliflower BoOr protein was expressed in the plastid of the leaf epidermal cells and the developing seeds[20], while the BoOR protein was also expressed in the nucleus in the young bud cells of transgenic Arabidopsis[58]. This study found that *ClOr1* could affect the *ClPSY1* expression level, similar phenomena have also been reported in Arabidopsis[47], which may be because there was a positive regulatory relationship between *ClOr1* and *ClPSY1*: the upregulation of *ClOr1* expression promoted the differentiation of chromoplast, which was equivalent to an increase in the storehouse of carotenoids accumulation, leading to the synthesis of more carotenoids. Therefore, the *ClPSY1* expression level would increase due to the increase in carotenoids. These results suggested that the *ClOr1* gene can positively influence the expression level of the *ClPSY1* gene in chromoplasts of watermelon flesh, thereby post-transcriptionally regulating the synthesis and accumulation of carotenoids. (Fig. 8, Supplementary Fig. S4).

Conclusions

This study provides new evidence for the role of the *ClOr1* gene in the regulation of carotenoid accumulation, chromoplast differentiation, and fruit coloration in plants. It was demonstrated that the *ClOr1* gene was highly expressed only in the ripe flesh of red-fleshed watermelon of the LSW-177, and was significantly correlated with carotenoid content. Overexpression of the *ClOr1* gene resulted in fruit coloration in transgenic tomato plants. TRV-mediated *ClOr1* gene silencing decreased carotenoid accumulation in the watermelon fruit flesh. Furthermore, the *ClOr1* combined with the *ClPSY1* promotes carotenoid accumulation. These results will provide insight into the gene function and molecular mechanism of the *ClOr1* gene to regulate carotenoid synthesis and accumulation during fruit development and ripening in watermelon, with the hope of promoting the genetic improvement of watermelon fruit flesh based on the *ClOr1* gene editing approaches in the future.

Author contributions

The authors confirm their contributions as follows: study design and manuscript revision: Zeng C, Wang P; investigation: Wang P, Zhou C; writing-original draft preparation: Zeng C, Zhou C; data curation: Tang Y, Zeng P; writing–review and editing: Amanullah S, Zhou Q, Zhu Q; project administration, supervision: Zhou Q, Zhu Q. All authors reviewed the results and approved the final version of the manuscript.

Data availability

All data generated or analyzed during this study are included in this published article and its supplementary information files.

Acknowledgments

This work was supported by the National Natural Science Foundation of China (Grant No. 31960607).

Conflict of interest

The authors declare that they have no conflict of interest.

Supplementary information accompanies this paper online at: https://doi.org/10.48130/vegres-0025-0049.

Dates

Received 3 September 2025; Revised 5 November 2025; Accepted 18 December 2025; Published online 9 February 2026

References

[1] Manivannan A, Lee ES, Han K, Lee HE, Kim DS. 2020. Versatile nutraceutical potentials of watermelon—a modest fruit loaded with pharmaceutically valuable phytochemicals. *Molecules* 25:5258

[2] Bangalore DV, McGlynn WG, Scott DD. 2008. Effects of fruit maturity on watermelon ultrastructure and intracellular lycopene distribution. *Journal of Food Science* 73:S222–S228

[3] Martin Ask N, Leung M, Radhakrishnan R, Lobo GP. 2021. Vitamin a transporters in visual function: a mini review on membrane receptors for dietary vitamin a uptake, storage, and transport to the eye. *Nutrients* 13:3987

[4] Alcaíno J, Baeza M, Cifuentes V. 2016. Carotenoid distribution in nature. In *Carotenoids in Nature*, ed. Stange C. Cham: Springer International Publishing. pp. 3–33 doi: 10.1007/978-3-319-39126-7_1

[5] Johnson EJ. 2014. Role of lutein and zeaxanthin in visual and cognitive function throughout the lifespan. *Nutrition Reviews* 72:605–612

[6] Yuan P, Umer MJ, He N, Zhao S, Lu X, et al. 2021. Transcriptome regulation of carotenoids in five flesh-colored watermelons (*Citrullus lanatus*). *BMC Plant Biology* 21:203

[7] Llorente B, Torres-Montilla S, Morelli L, Florez-Sarasa I, Matus JT, et al. 2020. Synthetic conversion of leaf chloroplasts into carotenoid-rich plastids reveals mechanistic basis of natural chromoplast development. *Proceedings of the National Academy of Sciences of the United States of America* 117:21796–21803

[8] Xu J, Wang X, Cao H, Xu H, Xu Q, et al. 2017. Dynamic changes in methylome and transcriptome patterns in response to methyltransferase inhibitor 5-azacytidine treatment in citrus. *DNA Research* 24:509–522

[9] Grassi S, Piro G, Lee JM, Zheng Y, Fei Z, et al. 2013. Comparative genomics reveals candidate carotenoid pathway regulators of ripening watermelon fruit. *BMC Genomics* 14:781

[10] Luo Z, Zhang J, Li J, Yang C, Wang T, et al. 2013. A STAY-GREEN protein SlSGR1 regulates lycopene and β-carotene accumulation by interacting directly with SlPSY1 during ripening processes in tomato. *New Phytologist* 198:442–452

[11] Ren Y, Han R, Ma Y, Li X, Deng C, et al. 2022. Transcriptomics integrated with metabolomics unveil carotenoids accumulation and correlated gene regulation in white and yellow-fleshed turnip (*Brassica rapa* ssp. *rapa*). *Genes* 13:953

[12] Kalladan R, Lasky JR, Sharma S, Kumar MN, Juenger TE, et al. 2019. Natural variation in 9-*cis*-epoxycartenoid dioxygenase 3 and ABA accumulation. *Plant Physiology* 179:1620–1631

[13] Chayut N, Yuan H, Saar Y, Zheng Y, Sun T, et al. 2021. Comparative transcriptome analyses shed light on carotenoid production and plastid development in melon fruit. *Horticulture Research* 8:112

[14] Liang MH, He YJ, Liu DM, Jiang JG. 2021. Regulation of carotenoid degradation and production of apocarotenoids in natural and engineered organisms. *Critical Reviews in Biotechnology* 41:513–534

[15] Yu H, Cui N, Guo K, Xu W, Wang H. 2023. Epigenetic changes in the regulation of carotenoid metabolism during honeysuckle flower development. *Horticultural Plant Journal* 9:577–588

[16] Rao S, Cao H, O'Hanna FJ, Zhou X, Lui A, et al. 2024. Nudix hydrolase 23 post-translationally regulates carotenoid biosynthesis in plants. *The Plant Cell* 36:1868–1891

[17] Chayut N, Yuan H, Ohali S, Meir A, Sa'ar U, et al. 2017. Distinct mechanisms of the ORANGE protein in controlling carotenoid flux. *Plant Physiology* 173:376–389

[18] Zhou X, Sun T, Owens L, Yang Y, Fish T, et al. 2023. Carotenoid sequestration protein FIBRILLIN participates in CmOR-regulated β-carotene accumulation in melon. *Plant Physiology* 193:643–660

[19] Fang X, Liu S, Gao P, Liu H, Wang X, et al. 2020. Expression of *ClPAP* and *ClPSY1* in watermelon correlates with chromoplast differentiation, carotenoid accumulation, and flesh color formation. *Scientia Horticulturae* 270:109437

[20] Lu S, Van Eck J, Zhou X, Lopez AB, O'Halloran DM, et al. 2006. The cauliflower or gene encodes a DnaJ cysteine-rich domain-containing protein that mediates high levels of β-carotene accumulation. *The Plant cell* 18:3594–3605

[21] Tzuri G, Zhou X, Chayut N, Yuan H, Portnoy V, et al. 2015. A 'golden' SNP in *CmOr* governs the fruit flesh color of melon (*Cucumis melo*). *The Plant Journal* 82:267–279

[22] Li L, Paolillo DJ, Parthasarathy MV, DiMuzio EM, Garvin DF. 2001. A novel gene mutation that confers abnormal patterns of β-carotene accumulation in cauliflower (*Brassica oleracea* var. *botrytis*). *The Plant Journal* 26:59–67

[23] Wang Z, Xu W, Kang J, Li M, Huang J, et al. 2018. Overexpression of alfalfa *Orange* gene in tobacco enhances carotenoid accumulation and tolerance to multiple abiotic stresses. *Plant Physiology and Biochemistry* 130:613–622

[24] Berman J, Zorrilla-López U, Medina V, Farré G, Sandmann G, et al. 2017. The Arabidopsis ORANGE (*AtOR*) gene promotes carotenoid

accumulation in transgenic corn hybrids derived from parental lines with limited carotenoid pools. *Plant Cell Reports* 36:933–945

[25] Yazdani M, Sun Z, Yuan H, Zeng S, Thannhauser TW, et al. 2019. Ectopic expression of *ORANGE* promotes carotenoid accumulation and fruit development in tomato. *Plant Biotechnology Journal* 17:33–49

[26] Kim SE, Lee CJ, Park SU, Lim YH, Park WS, et al. 2021. Overexpression of the golden SNP-carrying *Orange* gene enhances carotenoid accumulation and heat stress tolerance in sweetpotato plants. *Antioxidants* 10:51

[27] Zhang L, Zhang S, Dai Y, Wang S, Wang C, et al. 2022. Mapping and validation of BrGOLDEN: a dominant gene regulating carotenoid accumulation in *Brassica rapa*. *International Journal of Molecular Sciences* 23:12442

[28] Kang L, Zhang C, Liu J, Ye M, Zhang L, et al. 2023. Overexpression of potato ORANGE (StOR) and StOR mutant in *Arabidopsis* confers increased carotenoid accumulation and tolerance to abiotic stress. *Plant Physiology and Biochemistry* 201:107809

[29] Rodriguez GA. 2001. Extraction, isolation, and purification of carotenoids. *Current Protocols in Food Analytical Chemistry* F2.1.1–F2.1.8

[30] Arnon DI. 1949. Copper enzymes in isolated chloroplasts. polyphenoloxidase in *Beta Vulgaris*. *Plant Physiology* 24:1–15

[31] Xu R, Wang Y, Wang L, Zhao Z, Cao J, et al. 2023. PsERF1B-PsMYB10.1-PsbHLH3 module enhances anthocyanin biosynthesis in the flesh-reddening of amber-fleshed plum (cv. Friar) fruit in response to cold storage. *Horticulture Research* 10:uhad091

[32] Hu CD, Chinenov Y, Kerppola TK. 2002. Visualization of interactions among bZIP and Rel family proteins in living cells using bimolecular fluorescence complementation. *Molecular Cell* 9:789–798

[33] Kong Q, Yuan J, Gao L, Zhao S, Jiang W, et al. 2014. Identification of suitable reference genes for gene expression normalization in qRT-PCR analysis in watermelon. *PLoS One* 9:e90612

[34] Guo S, Zhao S, Sun H, Wang X, Wu S, et al. 2019. Resequencing of 414 cultivated and wild watermelon accessions identifies selection for fruit quality traits. *Nature Genetics* 51:1616–1623

[35] Jin B, Jang G, Park G, Shahwar D, Shin J, et al. 2024. Development of a gene-based marker set for orange-colored watermelon flesh with a high β-carotene content. *International Journal of Molecular Sciences* 25:210

[36] Tadmor Y, King S, Levi A, Davis A, Meir A, et al. 2005. Comparative fruit colouration in watermelon and tomato. *Food Research International* 38:837–841

[37] Ilahy R, Tlili I, Siddiqui MW, Hdider C, Lenucci MS. 2019. Inside and beyond color: comparative overview of functional quality of tomato and watermelon fruits. *Frontiers in Plant Science* 10:769

[38] Lv P, Li N, Liu H, Gu H, Zhao WE. 2015. Changes in carotenoid profiles and in the expression pattern of the genes in carotenoid metabolisms during fruit development and ripening in four watermelon cultivars. *Food Chemistry* 174:52–59

[39] Sun T, Yuan H, Chen C, Kadirjan-Kalbach DK, Mazourek M, et al. 2020. OR^{His}, a natural variant of OR, specifically interacts with plastid division factor ARC3 to regulate chromoplast number and carotenoid accumulation. *Molecular Plant* 13:864–878

[40] Bartley GE, Scolnik PA. 1995. Plant carotenoids: pigments for photoprotection, visual attraction, and human health. *The Plant Cell* 7:1027–1038

[41] Harris WM, Spurr AR. 1969. Chromoplasts of tomato fruits. I. Ultrastructure of low-pigment and high-beta mutants. Carotene analyses. *American Journal of Botany* 56:369–379

[42] Schweiggert RM, Steingass CB, Heller A, Esquivel P, Carle R. 2011. Characterization of chromoplasts and carotenoids of red- and yellow-fleshed papaya (*Carica papaya* L.). *Planta* 234:1031–1044

[43] Lado J, Zacarías L, Gurrea A, Page A, Stead A, et al. 2015. Exploring the diversity in *Citrus* fruit colouration to decipher the relationship between plastid ultrastructure and carotenoid composition. *Planta* 242:645–661

[44] Kim JE, Rensing KH, Douglas CJ, Cheng KM. 2010. Chromoplasts ultrastructure and estimated carotene content in root secondary phloem of different carrot varieties. *Planta* 231:549–558

[45] Sturaro M. 2025. Carotenoids in potato tubers: a bright yellow future ahead. *Plants* 14:272

[46] Morelli L, Torres-Montilla S, Glauser G, Shanmugabalaji V, Kessler F, et al. 2023. Novel insights into the contribution of plastoglobules and reactive oxygen species to chromoplast differentiation. *New Phytologist* 237:1696–1710

[47] Zhou X, Welsch R, Yang Y, Álvarez D, Riediger M, et al. 2015. *Arabidopsis* OR proteins are the major posttranscriptional regulators of phytoene synthase in controlling carotenoid biosynthesis. *Proceedings of the National Academy of Sciences of the United States of America* 112:3558–3563

[48] Gong C, Diao W, Zhu H, Umer MJ, Zhao S, et al. 2021. Metabolome and transcriptome integration reveals insights into flavor formation of 'Crimson' watermelon flesh during fruit development. *Frontiers in Plant Science* 12:629361

[49] Anees M, Gao L, Umer MJ, Yuan P, Zhu H, et al. 2021. Identification of key gene networks associated with cell wall components leading to flesh firmness in watermelon. *Frontiers in Plant Science* 12:630243

[50] Yu Y, Yu J, Wang Q, Wang J, Zhao G, et al. 2021. Overexpression of the rice *ORANGE* gene *OsOR* negatively regulates carotenoid accumulation, leads to higher tiller numbers and decreases stress tolerance in Nipponbare rice. *Plant Science* 310:110962

[51] Gao Y, Zhou X, Huang H, Wang C, Xiao X, et al. 2025. ORANGE proteins mediate adaptation to high light and resistance to *Pseudomonas syringae* in tomato by regulating chlorophylls and carotenoids accumulation. *International Journal of Biological Macromolecules* 306:141739

[52] Lopez AB, Van Eck J, Conlin BJ, Paolillo DJ, O'Neill J, et al. 2008. Effect of the cauliflower *Or* transgene on carotenoid accumulation and chromoplast formation in transgenic potato tubers. *Journal of Experimental Botany* 59:213–223

[53] Bai C, Capell T, Berman J, Medina V, Sandmann G, et al. 2016. Bottlenecks in carotenoid biosynthesis and accumulation in rice endosperm are influenced by the precursor–product balance. *Plant Biotechnology Journal* 14:195–205

[54] Oogo Y, Takemura M, Sakamoto A, Misawa N, Shimada H. 2022. Orange protein, phytoene synthase regulator, has protein disulfide reductase activity. *Plant Signaling & Behavior* 17:2072094

[55] Nie H, Kim M, Lee S, Lim S, Lee MS, et al. 2023. High-quality genome assembly and genetic mapping reveal a gene regulating flesh color in watermelon (*Citrullus lanatus*). *Frontiers in Plant Science* 14:1142856

[56] Liu S, Gao Z, Wang X, Luan F, Dai Z, et al. 2022. Nucleotide variation in the *phytoene synthase* (*ClPsy1*) gene contributes to golden flesh in watermelon (*Citrullus lanatus* L.). *Theoretical and Applied Genetics* 135:185–200

[57] Sun T, Zhou F, Huang XQ, Chen WC, Kong MJ, et al. 2019. ORANGE represses chloroplast biogenesis in etiolated Arabidopsis Cotyledons via interaction with TCP14. *The Plant Cell* 31:2996–3014

[58] Zhou X, Sun TH, Wang N, Ling HQ, Lu S, et al. 2011. The cauliflower *Orange* gene enhances petiole elongation by suppressing expression of *eukaryotic release factor 1*. *New Phytologist* 190:89–100